M. F. O. Schiefler Filho

Federal Center for Technological Education
Av. Sete de Setembro, 3165
80230-901 Curitiba, PR. Brazil
schiefle@cefetpr.br

A. J. A. Buschinelli

Federal University of Santa Catarina
Mailbox 476
88040-900 Florianópolis, SC. Brazil
buschi@emc.ufsc.br

**F. Gärtner, A. Kirsten, J. Voyer
and H. Kreye**

University of the Federal Armed Forces
Holstenhofweg 85
22043 Hamburg. Germany
frank.gaertner@unibw-hamburg.de

Influence of Process Parameters on the Quality of Thermally Sprayed X46Cr13 Stainless Steel Coatings

Thermally sprayed metallic coatings have been frequently applied over low carbon steel components, aiming at protecting against corrosion and wear. However, these coatings always contain pores, oxides and cracks in the microstructure, which affect the protection performance. The spraying process employed determines not only the amount and distribution of these defects, but also several coating properties (e.g. thickness, hardness and adhesion to the substrate). Therefore, the final coating quality is strongly related to the spray parameters definition, such as: fuel gas type, oxygen pressure, particle velocity and spray distance. This research aims at verifying the efficiency of the High Velocity Combustion Wire spray process (HVCW) for the deposition of X46Cr13 stainless steel coatings. This process submits the particles to higher velocities than those in conventional processes (e.g. flame spraying (FS) and arc spraying (AS)), normally producing more refined microstructures with better properties. The influence of spray parameters has been investigated considering characteristics of the microstructure and mechanical properties, as well as, with respect to the corrosion behavior in synthetic marine solution. The results have confirmed the favorable performance of the HVCW process, which has produced a sufficiently dense coating to prevent damages to the substrate. Additionally, the absorbed oxygen content has been considered adequate to obtain optimized mechanical properties, including wear resistance.
Keywords: Metallic coatings, thermal spraying, X46Cr13 stainless steel, corrosion, wear

Introduction

Low carbon and low-alloyed steel components are subjected to severe damage when operating in marine environments. This problem is normally found either due to electrochemical reaction (corrosion) or mechanical action (wear). Moreover, in the most of cases corrosion as well as wear occur simultaneously and begin at the surface of the components. Thus, a manner to block - or at least to delay – the progression of those detrimental phenomena is applying protective metallic coatings with suitable properties.

Among the commercial coating deposition techniques, thermal spraying (TS) is receiving much attention over the past years. It is a process in which the feedstock (e.g., metal, polymer or ceramic material) in the form of a powder, wire or rod is continuously fed and heated by a chemical or electrical heat source into a gun. At the same time, a gas stream accelerates the molten, semi-molten or solid particles and directs them onto a substrate surface, on which a coating is formed (Pawlowski, 1995). A major advantage of thermal spraying is the wide variety of materials which can be used.

It should be noted, however, that the microstructure of thermally sprayed coatings, which results from the solidification and sintering of the particles, frequently contain pores, oxides and cracks. The amount and distribution of these defects, as well as other coating properties as for instance thickness, hardness and bond strength, will be defined by the selected spray parameters. Therefore, the correct choice of the spray process as well as respective parameters (fuel gas type, particle velocity, spray distance and so on) is very important for the deposition of good coatings and, consequently, to enlarge the useful life in service of the components. Moreover, by using wires instead of spray powders of the same composition, the production costs for coatings are significantly smaller (Kreye et al., 2001). For that reason and in view of practical applications, the present study is focused on spray systems that use wires as feedstock.

The recently developed High Velocity Combustion Wire (HVCW) spray process can be a new alternative aiming at obtaining high quality coatings. This process imposes higher velocities to the sprayed particles, resulting in more refined microstructures which present better properties, in comparison to those obtained from conventional flame (FS) and electric arc (AS) processes.

In the case of corrosion, the protection mechanism associated to the coating depends on its electrochemical nobility. For coatings less noble with respect to the substrate (anodic coatings), the protection is based on the sacrificial effect (cathodic protection). For coatings more noble (cathodic coatings), the protection occurs when a physical barrier is created between substrate and corrosive environment (barrier protection).

Coating materials widely used in the cathodic protection of steels are aluminum, zinc, ZnAl and AlMg alloys. All these materials, however, do not show an acceptable wear resistance for most applications. On the other hand, cathodic materials as X46Cr13 stainless steel can simultaneously show good corrosion and wear resistances. However, they have a serious limitation as protective coatings, because any defect in their microstructure may allow the electrolyte to reach the substrate, and severe under-corrosion will take place at the latter, due to the large cathode/anode area ratio that will be created. Despite of that, coating materials presenting similar behavior such as AISI 316L stainless steel and Ni-based Hastelloy C-276 alloy have been much researched over the past years, for marine protection corrosion systems (Hofman et al., 1998; Eminoglu et al., 1999; Kuroda et al., 2000; Sturgeon, 2001 and Schiefler et al., 2002).

The aim of the present paper was verify the potentiality of the HVCW process for spraying X46Cr13 stainless steel coatings, in order to promote the protection of low carbon steel substrates against corrosion and wear in marine environments. For that purpose, the performance of different spray systems and their respective parameters were compared. Conventional flame and arc sprayed coatings were also tested,

allowing an additional comparison among processes. The influence of the spray conditions was analyzed based on the microstructural characteristics and properties obtained, as well as on the corrosion behavior as immersed in synthetic marine solution.

Nomenclature

AS = Arc Spraying
CE = Counter Electrode
DS = Double Stroke
E_{corr} = Corrosion Potential or Open Circuit Potential (OCP), mV
EDS = Energy Dispersive Spectroscopy
FS = Flame Spraying
$HVCW$ = High Velocity Combustion Wire Spraying
I_{corr} = Corrosion Current, μA
i_{corr} = Corrosion Current Density, $\mu A/cm^2$
OM = Optical Microscopy
PAP = Potentiodynamic Anodic Polarization Test
R_a = Roughness, μm
RE = Reference Electrode
Rp = Polarization Resistance or Linear Polarization, $k\Omega.cm^2$
SCE = Standard Calomel Electrode
SEM = Scanning Electron Microscopy
TS = Thermal Spraying
WE = Working Electrode

Materials and Methods

Preparation of Coatings

Prior to deposition of the DIN X46Cr13 stainless steel coatings, DIN St 37 low carbon steel substrates (1.0038, nominally 50x70x4 mm^3 in size) were degreased and then grit-blasted with 0.1-1.0 mm alumina particles. For flame (FS) and arc (AS) spraying, a Metco 10 E system from Sulzer Metco, Westbury, NY, USA and a Tafa 9000 system from Tafa, Concord, NH, USA were used, respectively. HVCW spraying was performed with the W 1000 system from Metatherm GmbH, Homburg, Germany, or the HVw 2000 system from High Velocity Technologies Inc., West Lebanon, NH, USA. Their operation principles are schematically exhibited in Fig. 1.

The approximate chemical composition of the coating material is given in Table 1, whereas Table 2 summarizes the spray systems and parameters related to all investigated specimens.
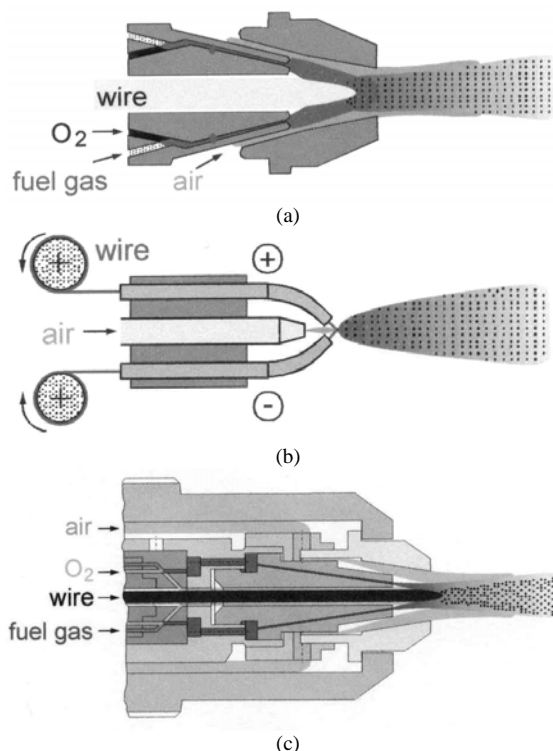

(a)

(b)

(c)

Figure 1. Operation principles of the thermal spray systems used in this investigation. (a) Flame Spraying (FS); (b) Arc Spraying (AS); (c) High Velocity Combustion Wire Spraying (HVCW).

Table 1. Approximate chemical composition of the coating material.

X46Cr13	C	Cr	Si	Mn	P	S	Fe
wt. %	0.46	13.5	1.0	1.0	≤ 0.040	≤ 0.015	Bal.

Table 2. Thermal spray systems and respective parameters.

Specimen	FS	AS	HW1	HW2	HW3	HW4
Spray System	Metco 10E	Tafa 9000	W 1000	W 1000	HVw 2000	HVw 2000
Wire Diameter (mm)	3.16	1.60	1.60	3.20	1.60	1.60
Wire Feed Rate (m/min)	0.48	--	0.60	0.37	1.60	2.80
Spray Distance (mm)	130	150	150	215	150	220
Number of Passages	4	12	14	10	10	6
Fuel Gas (bar / l/min)	Acetylene / 19	-- --	Propane 3.4 / 35	Propane 3.5 / 36	Propane 3.8 / 22	Ethylene 3.9 / 33
Oxygen (bar / l/min)	/ 43	--	2.1 / 55	7.0 / 179	4.1 / 103	2.0 / 95
Compressed Air (bar / l/min)	/ 775	4.1 /	5.0 / 464	6.5 / 603	6.6 / 551	6.1 / 513
Potential (V)	--	30	--	--	--	--
Current (A)	--	150	--	--	--	--
Cooling	--	--	--	Air/CO_2	--	--

FS = Flame Spraying; AS = Arc Spraying; HW (HVCW) = High Velocity Combustion Wire Spraying

Metallographic Preparation and Microscopic Analysis

Metallographic samples were prepared from coated specimens. Basically, the experimental procedure was composed of the following steps: (a) application of a protective resin on the surface to be analyzed; (b) cross sectioning using abrasive wheel by a Struers equipment model Discotom-2; (c) embedding of the samples in cold mounting resin; (d) automatic grinding with abrasive papers (grits 320, 500 and 1000), according to specific routine developed for Struers equipment model RotoPol-31; (e) automatic polishing of the samples by the same equipment, using diamond suspensions with grain sizes of 6, 3, 1 and 0.25 μm.

After preparation, the different morphologies of the various coatings were analyzed by optical microscopy (OM) using a Leica microscope model DM, which was equipped with camera and video systems. Further analyses were performed on a selected coating using a scanning electron microscope (SEM) from Philips model XL-40, as well by energy dispersive spectroscopy (EDS) using a Vantage digital microanalysis system from Noran Instruments, whose goal was to semi-quantify the chemical composition of the coating before and after corrosion test.

Microstructural Characterization and Mechanical Properties

The measurements of thickness were carried out on polished cross sections of the specimens, by using optical microscopy (OM). The images were displayed on a video monitor and the values were taken from a digital measurement system. The oxygen content of the coatings was determined by the inert gas fusion technique, using a Leco TC-436-DR equipment. The coating porosity was determined by quantitative image analysis on the basis of optical micrographs taken from cross sections at magnifications of 100X or 500X, depending on the thickness of the specimen. The surface roughness was measured by a digital equipment from Taylor Hobson, model Surtronic 3+, according to standard DIN 4768.

Microhardness tests were conducted in accordance to the standard DIN 50133, using a Vickers diamond pyramid indenter from Leitz. The measurements were performed with a load of 2,94 N (300 gf) on polished cross sections of the specimens. The bond strength of coatings was tested according to standard DIN EN 582, in which cylinders of 25 mm diameter were coated on one side, glued to a grit blasted counter body and pulled apart in a tensile testing machine. Finally, the wear tests were performed in accordance to the Japanese standard JIS H 8615. As output value, the mass loss after 1200 double strokes was taken.

Electrochemical Characterization

The corrosion behavior of the coatings was valued by monitoring the corrosion potential (E_{corr} vs. t), as well as by polarization resistance (Rp) and potentiodynamic anodic polarization (PAP) tests. All experiments were set up in freshly prepared synthetic marine solution, i.e. a 1 mol/l NaCl electrolyte. These tests were conducted after subsequently cleaning the specimens with purified water, degreasing them with ethanol in an ultrasonic bath and final drying under hot air stream. A part of the coatings were also tested in two different conditions: as-sprayed and as-sprayed + detached from the substrate. For comparison, also experiments were performed for bulk materials of St 37 low carbon steel (sheet) and X46Cr13 stainless steel (wire). In both cases, the specimens were grinded down to grit size 1000 and cleaned using the same procedure described above.

Immersion tests (E_{corr} vs. t) were carried out for a total duration of 96 hours and the electrochemical cells consisted of a simple two-electrode arrangement, where the specimen had the hole of working electrode (WE) and an Ag/AgCl (KCl sat.) electrode served as reference (RE). The assembled cells were filled with the electrolyte and closed inside a Faraday shield, equipped with a ventilation system. In addition, the inside temperature was controlled to a set point of 30 ± 1ºC. Throughout the tests, potential and temperature values were automatically stored on a computer with a sampling rate of 1/60 Hz. The exposed area of the specimens was 2 cm^2 and the experiment configuration allowed simultaneous testing of three cells.

The electrochemical cells used in the polarization experiments consisted of a three electrode arrangement (flat cell model K0235 from EG&G, Princeton, USA). Measurements were conducted at room temperature with a commercial potentiostat and commercial software

(model 273a and version 352 SoftCorr III, respectively, both from the same manufacturer). The specimen area exposed to the electrolyte was 1 cm^2 and the open potential (E_{corr}) relative to a SCE reference electrode was continuously monitored over a stabilisation period of 1 hour. For the polarization resistance (Rp) tests, the specimens were then potentiodynamically polarized to a range of -25 mV $\leq E_{corr} \leq$ +25 mV at a rate of 0.167 mV/s, while measuring the corrosion current (I_{corr}) with respect to a platinum wire mesh as counter electrode (CE). For comparison, Rp measurements were also carried out after the 96 h potential monitoring tests. The potentiodynamic anodic polarization (PAP) tests were performed in a similar manner, but to a much more wide polarization range (from -250 mV $\leq E_{corr}$ to -100 mV).

Results and Discussion

The results from microstructural characterization and mechanical properties measurements, which were obtained for the different coatings, are presented and compared in Table 3. It can be observed that the spray parameters used for each specimen (as indicated in Table 2) leaded to coatings having comparable mean thickness values (maximal variation of about 60 μm). This fact has facilitated the subsequent analyze of the others coating characteristics and properties.

Table 3. Results in terms of microstructural characterization and mechanical properties.

Specimen	FS	AS	HW1	HW2	HW3	HW4
Thickness (μm)	270 ± 15	288 ± 18	245 ± 20	305 ± 35	300 ± 30	303 ± 13
Oxygen Content (wt. %)	1.87 ± 0.02	4.26 ± 0.10	8.55 ± 0.28	11.38 ± 0.19	2.10 ± 0.01	4.52 ± 0.12
Porosity* (vol. %)	3.5	4.0	2.0	3.0	3.0	3.0
Roughness, R_a (μm)	14.4 ± 0.8	14.7 ± 1.2	13.4 ± 1.3	9.6 ± 1.5	13.9 ± 2.8	11.7 ± 1.3
Hardness (HV0.3)	392 ± 42	315 ± 38	570 ± 39	387 ± 53	387 ± 31	446 ± 20
Bond Strength (MPa)	56.8 ± 3.6	40.1 ± 2.2	76.9 ± 8.8	34.7 ± 4.9	29.7 ± 3.1	39.6 ± 2.4
Mass Loss* (mg/1200 DS)	104.6	111.3	91.0	119.0	104.2	94.6

* Mean values

FS = Flame Spraying; AS = Arc Spraying; HW (HVCW) = High Velocity Combustion Wire Spraying

On the other hand, the absorbed oxygen contents have varied significantly (i.e., from approximately 1.9 to 11.4 wt. %). It is commented in various publications (Kreye, 1997; Neiser et al., 1998 and Gourlaouen et al., 2000) that the oxygen absorption followed by particle oxidation can occur in different steps, in the case of processes that use flame: (a) in the "core" region of the flame, where oxygen is made available by the combustion products; (b) by interaction with the ambient atmosphere that penetrates in the flame, during the "fly time" of the heated particles until their impact upon the substrate; (c) after impact, during cooling of the particles recently sprayed on the substrate. Recently Dobler et al. (2000) have published that the contribution of these different oxidation steps to the oxygen content of a coating depends not only upon the spray parameters, but also on the spray metal feedstock.

With respect to HW2 specimen, for example, the greater oxygen/propane rate used (see values in Table 2) was one of the factors that have caused the high content of absorbed oxygen (11.38%) – situation related to step (a). Besides that, a longer spray distance (215 mm) – situation related to step (b), the high flow of compressed air (603 l/min) and the additional cooling using air/CO_2 – situation related to step (c), have also contributed to elevate the oxygen content of the coating.

As expected, the slight lower porosity present in HVCW coatings, in comparison to FS and AS coatings, has originated from the higher velocity imposed to the particles by the former spray process. Among all coatings, HW1 has showed the lowest mean porosity (2%).

The roughness measurements have indicated similar values for the most coatings. The lower mean roughness of the HW2 coating (9.6 μm) has resulted, possibly, from the longer spray distance used in that case (215 mm, as seen in Table 2). Additionally, the HW4 coating, which was also sprayed from a longer distance (220 mm, as seen in Table 2), has presented the second lower roughness (11.7 μm).

The graphs in Fig. 2 illustrate the influence of oxygen content on the measured mechanical properties, for all X46Cr13 HVCW sprayed coatings.
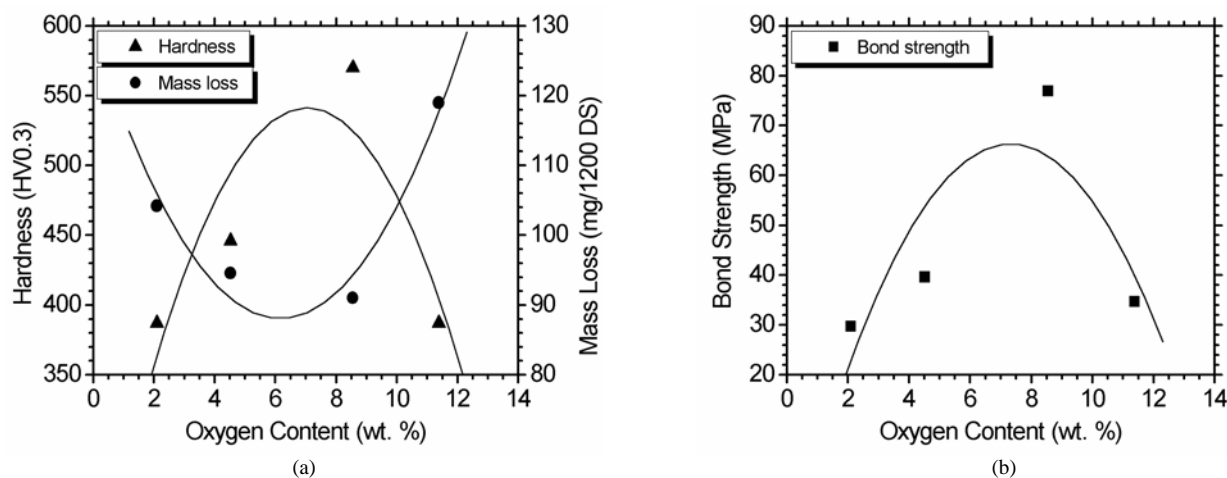

(a)

(b)

Figure 2. Influence of oxygen content on the mechanical properties of the investigated HVCW sprayed coatings. (a) Hardness and wear resistance (mass loss); (b) Bond strength.

It can be noted in Fig. 2 that the oxygen content of HW1 coating (8.55%, as seen in Table 3) is localized on the same region where hardness, wear resistance and bond strength are exhibiting optimized values. The relatively low oxygen content present in HW3 coating (only 2.10%) could be seen as insufficient to assure adequate mechanical properties. On the other hand, the quite elevated oxygen value present in HW2 coating (11.38%) has demonstrated excessive to keep its mechanical integrity.

Interestingly, the hardness measurements performed for these two coatings has indicated the same value (387 HV0.3, as seen in Table 3). Among the coatings, AS showed the lowest hardness (315 HV0.3), which could be related to a greater presence of different defects in its microstructure (mainly cracks). Another factor of influence could be the operation temperature of the AS process, which is considerably higher than the ones of the processes using flame. This higher temperature would generate a greater alloy elements-depletion (mainly chromium) during the coating deposition process.

The bar graphs in Fig. 3 are comparing corrosion potentials (E_{corr}) and polarization resistances (Rp) after 1 and 96 hours immersion, as showed below. In this case, the potential values were changed from "E_{corr} vs. Ag/AgCl (KCl sat.)" to "E_{corr} vs. SCE", aiming at facilitating the analyses.

(a)   (b)
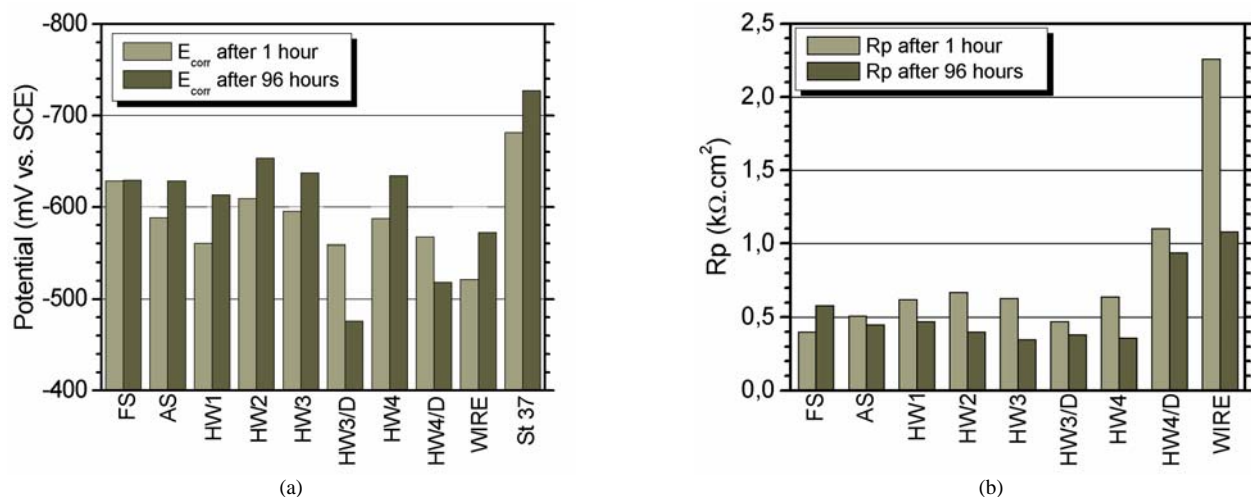
Figure 3. (a) E_{corr} values reached by various X46Cr13 stainless steel coatings, X46Cr13 wire and St 37 steel substrate, after 1 and 96 hours immersion; (b) Corresponding Rp values. HW3/D and HW4/D represent coatings tested after detachment from the substrate.

Relevant information that is obtained from E_{corr} vs. t tests is the relative difference between coating and substrate potentials, which can reveal possible galvanic interactions. In addition, the recovering degree of the substrate can be estimated comparing different behaviors demonstrated by coated and uncoated specimens.

The potentials showed by X46Cr13 wire and all coatings were less negative in comparison to the potential of the St 37 substrate, confirming the greater electrochemical nobility of the stainless steel (as observed in Fig. 3a). In the case of the values measured after 1-hour immersion, the potentials of the coatings for any condition were more negative than the potential of the bulk wire. That is, by the thermal spray process it has occurred a lack of the barrier-protective capacity of the material. It can be also noted that the potentials of the wire and coatings (except for HW3/D and HW4/D) have became more negative for 96 hours immersion. Among those coatings, HW1 has remained more positive (that is, more distant with respect to the potential of the substrate). At the same time, the potentials of the coatings detached from the substrate (i.e., HW3/D and HW4/D) have migrated to more positive values, even when compared to the potential of the wire. This behavior indicates that both coatings can be experimented passivation during immersion in the electrolyte. E_{corr} of FS coating, after it has became more negative along the test, has came back to the value initially measured after 96 hours immersion.

The purpose of Rp experiments, as summarized in Fig. 3b, was to determine the protection capacity of the coatings, which is made by measuring the oxidation resistance during the incidence of an external potential. The results indicate that all X46Cr13 sprayed coatings show lower Rp values than the original bulk material (wire), independently of the spray process used. The appearance of microstructural defects during the deposition process is, probably, the cause for this significant loss in Rp. Except for FS, the coatings have had a decrease in Rp and, consequently, an increase in corrosion current (I_{corr}) over the test time. This behavior suggests that the time of 96 hours immersion was insufficient to allow the development of a passive protective film on the surface contacting the electrolyte, which conflicts in any way with the potential monitoring (E_{corr} vs t) results presented for HW3/D and HW4/D coatings. Rp for HW4/D was localized very near the value reached by the bulk wire (≈ 1 kΩ.cm^2), whereas Rp for HW4 has became very similar to the values obtained by the other coatings.

This fact leads to believe that the electrolyte has really reached the substrate, influencing in this way the value of Rp.

Interestingly, that difference was not observed between HW3/D and HW3.

Optical micrographies of the several investigated coatings in the as-sprayed condition, as well as after 96 hours immersion by E_{corr} vs. t tests can be compared in Fig. 4. As it can be easily observed from the pictures, the choice of different spray parameters (as indicated in Table 2) has promoted significant modifications in the microstructures and morphologies of the coatings, which has confirmed the great variation of results showed in Table 3.

The different oxygen contents, for instance, have directly reflected on the relative amount of the formed oxides (gray phase), according to showed in the micrographies of Figs. 4e, 4f, 4c and 4d. The corresponding microstructures contain, respectively, increasingly quantities of oxygen. The two first pictures (4e and 4f) also illustrate the typical lamellar structure of thermally sprayed coatings. HVw 2000 system seems that has generated, therefore, less refined microstructures than W 1000 system.

The micrographies presented in Figs. 4a', 4b', 4e' and 4f', which were obtained after the immersion tests, are showing a severe corrosive attack of the substrate at its interface with the more noble coating. Apparently, such attack has not occurred for HW1 (as seen in Fig. 4c'). Although Fig. 4d shows a region containing high concentration of defects, which is localized from the HW2 coating edge up to its interface with the substrate, the corrosive attack on the latter seems not so aggressive (as seen in Fig. 4d').

Complementing the electrochemical tests which were presented in Fig. 3, Figure 5 exhibits potentiodynamic anodic polarization (PAP) curves obtained for coatings, wire and substrate materials. It is demonstrated in Fig. 5a that all coatings have demonstrated E_{corr} more negative than X46Cr13 steel as bulk material. These results, which are in accordance with the data showed in Fig. 3, have reflected again the important microstructural changes already presented in Fig. 4. Moreover, recent work (Schiefler et al., 2002) explains that a similar situation has been already observed for AISI 316L stainless steel and Ni-based Hastelloy C-276 coatings, which were sprayed on the same DIN St 37 low carbon steel substrate.
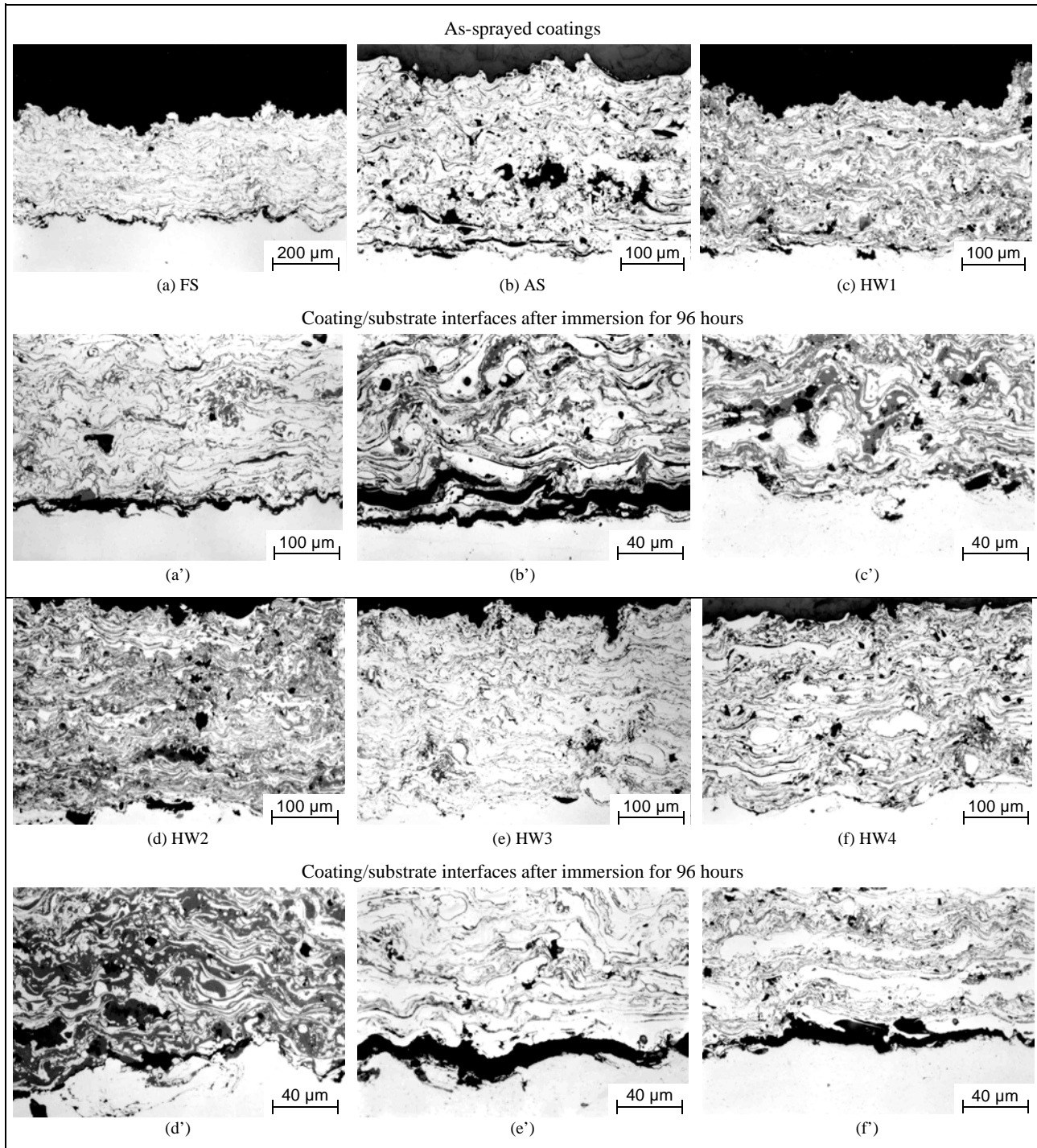

Figure 4 (Part 2). Optical micrographies of investigated X46Cr13 steel coatings, before (d-f) and after (d'-f') the E_{corr} vs. t test for 96 hours.

Among all coatings, HW1 has showed E_{corr} ($\approx$ -575 mV) more distant from the potential of the substrate ($\approx$ -685 mV) and, at the same time, closer to the potential of the X46Cr13 bulk wire ($\approx$ -525 mV). That behavior suggests a higher capacity to promote barrier protection, whereas in opposite the more negative E_{corr} was presented by the coating sprayed by FS ($\approx$ -630 mV). No coatings have clearly demonstrated ability to passivation, but HW1 and AS beside the wire have exhibited a small tendency to this phenomenon.

Figure 5b also includes polarization curves for HW3 and HW4 coatings after their detachment from the substrate, which are indicated by HW3/D and HW4/D, respectively. Once eliminated the direct contact with the substrate, both coatings have presented E_{corr} more positive and consequently closer to the corrosion potential of the wire, as well as some tendency to passivation. Therefore, it can be assumed that the potentials measured for HW3 and HW4 coatings are, in really, mixed corrosion potentials derived from coating and substrate.
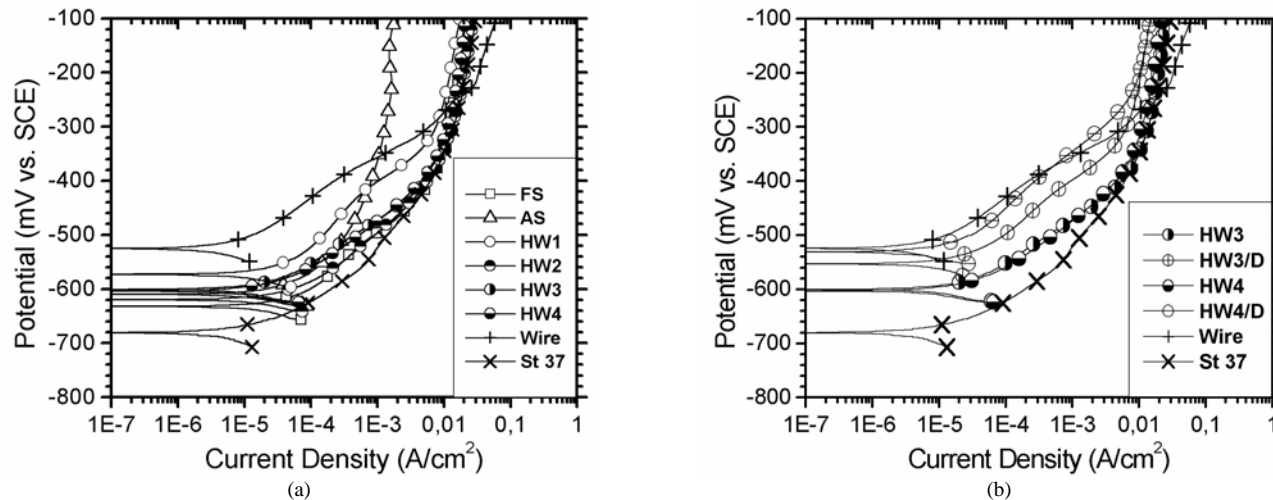

Figure 5. (a) Comparison among PAP curves for different X46Cr13 coatings, X46Cr13 bulk wire and St 37 steel substrate. (b) Positive displacement of E_{corr} as occurred for HW3/D and HW4/D coatings.

This fact confirms that the electrolyte really reaches the substrate, permeating through the defects present in the coating microstructures, as already illustrated in the micrographies of Figs. 4e' and 4f'. The same case should have also occurred for FS, AS and HW2. The behavior of the potential of HW1, as describe above, would justify the absence of corrosive attack (as seen in Fig. 4c').

The results obtained up to now have indicated HW1 as the more suitable coating, not only concerning corrosion protection but also in terms of abrasive wear protection. Thus HW1 was selected and then further analyzed by scanning electron microscopy (SEM), aiming at assessing the possible corrosion mechanisms which are acting. The micrographies presented in Fig. 6 illustrate the polished surface of this coating before (a) and after (b-f) it was submitted to a potentiodynamic anodic polarization test.
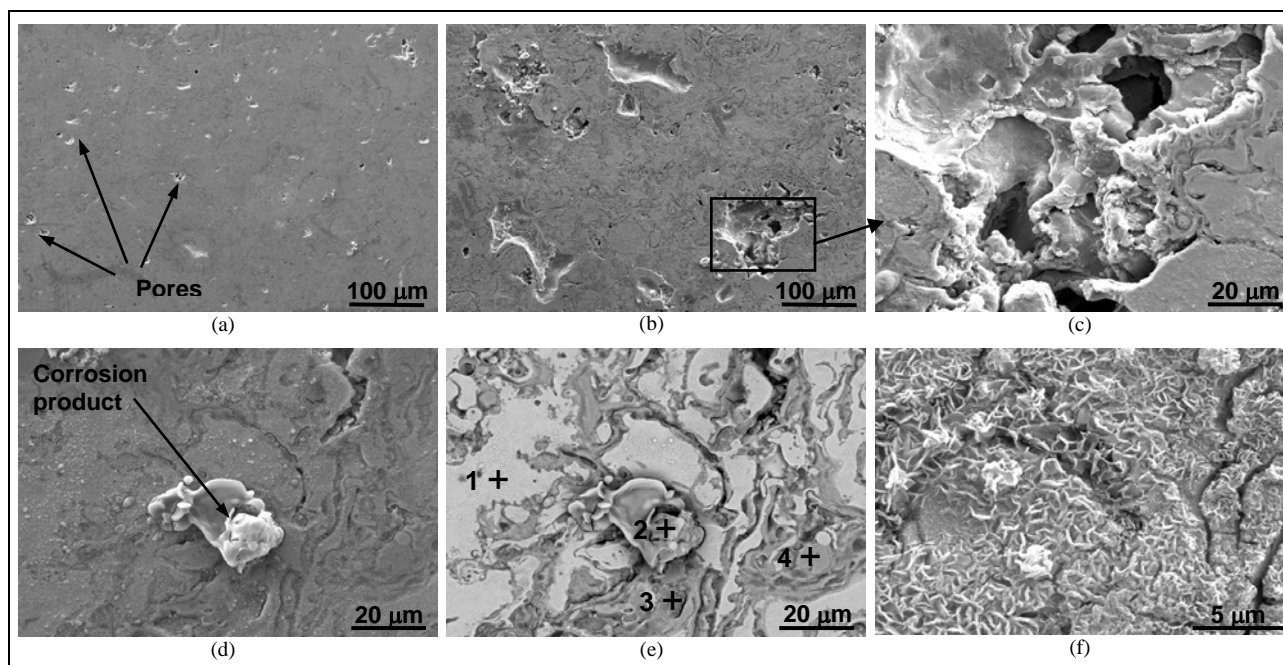

Figure 6. SEM micrographies of HW1 coating. (a) Thermally sprayed surface after polishing and before PAP testing; (b) Corroded surface after testing; (c) Close up from the previous image; (d) Corrosion product (SE method); (e) Previous image (BSE method) indicating the points of EDS analyzes; (f) Morphology of the corroded surface.

Figure 6a reveals a low porosity, which was estimated as 2% in volume as referred in Table 3. Based on the micrography presented in Fig. 4c', that porosity is supposedly not interconnected, because it has not permitted that the substrate had been reached by the electrolyte for 96 hours immersion. A general view of the corroded surface after test, which is exhibited in Fig. 6b, suggests that the attack of the electrolyte was more intense on certain regions (i.e., localized corrosion), normally associated to pre-existing defects. Fig. 6c contains a close up from Fig. 6b, which clearly shows that the localized corrosive attack can be very deep, reaching even many layers of the coating. Figures 6d and 6e in turn exhibit a corrosion product which has formed on the surface. The former was taken by using SE (Secondary Electrons) method and the latter was taken by using BSE (Back-Scattering Electrons) one. These detection methods should be used if it is desirable a great focus depth and a sharply defined phase contrast, respectively. On Fig. 6e are indicated the points where the EDS analyses were carried out aiming at qualifying the chemical composition, whose values can be compared in the following Table 4. Finally, the rather great enlargement presented in Fig. 6f allows observing the typical morphology of the corroded surface. It can be also noted based on Figs. 6d and 6f that the corrosive attack occurs preferentially at the interface oxide/metallic phase. Table 4 presents EDS analyses performed on specific regions and points of the HW1 coating.

Table 4. EDS analyses of chemical composition obtained for HW1 coating.

Composition (wt. %)	Cr	Si	Mn	O	Cl	Na	Fe
Non-corroded Region	12.6	1.2	0.2	10.9	--	--	Bal.
Corroded Region	16.5	1.3	0.2	21.9	0.5	--	Bal.
Point 1*	13.5	1.3	0.4	11.9	0.2	--	Bal.
Point 2*	3.4	0.7	0.1	41.0	4.2	0.2	Bal.
Point 3*	22.7	0.9	0.4	30.4	1.1	--	Bal.
Point 4*	17.2	0.8	--	39.2	0.2	--	Bal.

* These points are indicated on the corroded surface presented in Figure 6e.

Unfortunately, EDS analyze method has a limited capability to estimate the content of light elements, such as carbon and oxygen. In the case of the first one, the content could not be measured with acceptable values, whereas for the second one, its value attributed in Table 4 (10.9%) appears increased in comparison to the earlier mentioned more accurate value (8.55%, as seen in Table 2). This discrepancy has not prevented, however, a qualitative analyze of the obtained results. The relatively greater content of chromium identified on a corroded region (surface showed in Fig. 6b), in comparison to a non-corroded region (surface showed in Fig. 6a), probably results from a indirect effect caused by the iron fraction which was lost during its selective corrosion. It can be additionally observed that the oxygen content is twice as much in the corroded region, whereas silicon and manganese contents have remained practically unchanged. Concerning punctual analyses, point 1 is localized on the metallic phase and its composition appears very similar to that measured on the non-corroded region. Point 2 is exactly localized on a corrosion product which was generated during the PPA test. As expected, that substance is rich in oxygen and poor in chromium, besides to contain chlorine and sodium traces, whose composition supposedly belongs to $Fe(OH)_2$.

On the other hand, the points 3 and 4 were measured on darkened areas of the microstructure, which are oxygen- and chromium-enriched areas containing, in addition, variable amounts of chlorine. In spite of carbon content was not estimated, their values presented in Table 4 suggest that there is a coexistence of chromium-oxide and chromium-carbide, which were not distinguishable themselves from the details showed in the figure.

Conclusions

The variation of spray parameters adopted in the present investigation has had a great influence on the quality of X46Cr13 stainless steel coatings. This fact could be demonstrated by the large variation obtained in terms of microstructural characteristics, mechanical properties and corrosion performance.

Considering the spray conditions indicated in Table 2, the High Velocity Combustion Wire (HVCW) process has permitted the deposition of a coating having better quality (i.e., HW1 coating) as compared to the other ones, which were deposited by conventional FS and AS spray processes.

The different oxygen contents, which were absorbed as a function of the various spray parameters, have allowed identifying a value range where the mechanical properties are optimized. The oxygen content present in HW1 coating has localized inside that range.

Based on the obtained results, W 1000 spray system (HVCW) would be the recommended one, operating with the following process parameters: wire diameter of 1.60 mm and feed rate of 0.60 m/min, spray distance of 150 mm with 14 passages and gas flow of 35/55/464 l/min (respectively for propane, oxygen and compressed air).

Curiously, HW1 coating has showed the thinner thickness (245 μm, as seen in Table 3). The others microstructural characteristics and properties obtained were: oxygen content of 8.55 wt.%, porosity of 2.0 vol. %, roughness (R_a) of 13.4 μm, microhardness of 570 HV0.3, bond strength (adherence to the substrate) of 76.9 MPa and mass loss (wear) of 91.0 mg/1200DS.

The used electrochemical techniques (i.e., E_{corr} vs. t, Rp and PAP tests) have been very useful to investigate the corrosion behavior of the different coatings. Apparently, HW1 coating was the only one able to prevent the corrosive attack of the substrate at the coating/substrate interface. Among all studied coatings, HW1 coating has presented the nearest corrosion potential with respect to the one of the bulk material (wire). At the same time, that potential is the most distant from the corrosion potential of the substrate, and both situations mentioned above are meaning a greater ability to promote barrier protection. All as-sprayed coatings have showed a low polarization resistance (Rp) and lack of significant passivation in the electrolyte (synthetic marine solution). On the other hand, for HW3/D and HW4/D coatings there was light tendency to passivation.

SEM and EDS analyses carried out on HW1 coating have facilitated the understanding of the possible corrosion mechanisms that are occurring in thermally sprayed X46Cr13 stainless steel coatings.

Acknowledgements

References

Dobler, K., Kreye, H. and Schwetzke, R., 2000, "Oxidation of Stainless Steel in the High Velocity Oxy-Fuel Process", Journal of Thermal Spray Technology, V. 9, No. 3, pp. 407-413.

Eminoglu, C.M., Knight, R., DeFalco, J. and Dorfman, M., 1999, "Potentiodynamic Corrosion Testing of HVOF Sprayed Stainless Steel Alloy", Proceed. of the United Thermal Spray Conference (UTSC 99), Düsseldorf, Germany, pp. 39-44.

Gourlaouen, V., Verna, E. and Beaubien, P., 2000, "Influence of Flame Parameters on Stainless Steel Coatings Properties", Proceed. of the 1st International Thermal Spray Conference (ITSC 2000), Montréal, Québec, Canada, pp. 1011-1015.

Hofman, R., Vreijling, M.P.W., Ferrari, G.M. and De Wit, J.H.W., 1998, "Electrochemical Methods for Characterisation of Thermal Spray Corrosion Resistant Stainless Steel Coatings", Materials Science Forum, Vols. 289-292, pp. 641-654.

Kreye, H., 1997, "Vergleich der HVOF-Systeme – Werkstoff-verhalten und Schichteigenschaften", Proceed. of the 4. Kolloq. Hochgeschwindigkeits-Flammspritzen, Erding, Germany, pp. 13-21.

Kreye, H., Kirsten, A., Gärtner, F., Qi, X. and Krömmer, W., 2001, "High Velocity Combustion Wire Spraying - Systems and Coatings", Proceed. of the International Thermal Spray Conference (ITSC 2001), Singapore, pp. 461-466.

Kuroda, S., Fukushima, T., Kodama, T. and Sasaki, M., 2000, "Microstructure and Corrosion Resistance of HVOF Sprayed 316L Stainless Steel and Ni Base Alloy Coatings", Proceed. of the 1st International Thermal Spray Conference, Montréal, Canada, pp. 455-462.

Neiser, R.A., Smith, M.F. and Dykhuizen, R.C., 1998, "Oxidation in Wire HVOF-Sprayed Steel", Journal of Thermal Spray Technology, ASM International, V. 7, No. 4, pp. 537-545.

Pawlowski, L., 1995, "The Science and Enginnering of Thermal Spray Coatings", John Wiley & Sons Ltd, England, 1995, 414p.

Schiefler Fo, M.F.O., Voyer, J., Gärtner, F. and Qi, X., 2002, "Corrosion Behaviour of High Velocity Combustion Wire Sprayed Coatings", Proceed. of the International Thermal Spray Conference (ITSC 2002), Essen, Germany, pp. 553-558.

Sturgeon, A.J., 2001, "Microstructure Characteristics and Corrosion Behaviour of HVOF Sprayed Metallic Coatings", Proceed. of the Int. Thermal Spray Conference, Singapore, pp. 1149